Ultrathin electrospun PANI nanofibers for neuronal tissue engineering

R. Castagna,[1,2] M. Tunesi,[1,2] B. Saglio,[1,3] C. Della Pina,[4] A. Sironi,[4] D. Albani,[5] C. Bertarelli,[1,2]

E. Falletta[4]

1 Dipartimento Di Chimica, Materiali E Ingegneria Chimica "G. Natta," Politecnico Di Milano, Piazza L. Da Vinci 32, Milano 20133, Italy
2 Italian Interuniversity Consortium on Material Science and Technology, INSTM, UdR Milano Politecnico, via G. Giusti 9, Firenze 50121, Italy
3 Center for Nano Science and Technology @PoliMi, Istituto Italiano Di Tecnologia, via Pascoli 70/3, Milano 20133, Italy
4 Dipartimento Di Chimica, Universita Degli Studi Di Milano, CNR-ISTM, via Golgi 19, Milano 20133, Italy
5 Department of Neuroscience, IRCCS- Istituto Di Ricerche Farmacologiche "Mario Negri," via La Masa 19, Milan 20156, Italy
Correspondence to: E. Falletta (E-mail: ermelinda.falletta@unimi.it)

Received 23 December 2015; accepted 29 April 2016

INTRODUCTION

Nonwovens nanofibers, an innovative class of engineered textiles and fabrics, are being witnessed to a rapid growing market thanks to their numerous and different applications in many fields, such as electromagnetic interference shielding,[1] electrostatic charge dissipation,[2] materials corrosion,[3] rechargeable batteries,[4] solar cells,[5] and chemical sensors.[6] Nanofiber-based matrices have also demonstrated potential application as scaffolds in regenerative medicine. Owing to the high surface to volume ratio, nanofibers enhance sensitivity[7] with respect to the bulk; furthermore, together with their porous structure, they provide a larger and suitable substrate for cell attachment and improve cell proliferation, migration, and differentiation.[8]

Among the materials that can be produced as nanofibers, intrinsically conducting polymers (ICPs, e.g., polypyrrole, polythiophene, polyaniline [PANI], poly(3,4-ethylenedioxythiophene)) take a special place for their extraordinary properties. They have been recently investigated in the field of skeletal, cardiac, and nerve tissue engineering. In particular, it has been found that electrical stimulation is an effective cue to modulate neuronal cell adhesion and proliferation while enhancing neurite and axonal formation.

Scaffold porosity is indeed an important issue in scaffold-design, since it can influence cell migration, tissue growth, oxygen, nutrient, signaling molecule diffusion and waste removal.[9,10] However, the prediction and control over the porous structure of the electrospun mat is not always trivial, due to the complexity of the

fiber spinning process. Recently, a theory for estimating pore size distribution has been proposed and experimentally validated.[11,12] Nowadays, efforts are pointed towards the creation of 3D porous scaffolds with a good penetration depth of cells and controlled pore size. Electrospun mats with high porosity for cell infiltration and migration are desired and fibers mimicking the dimension (lower than 100 nm in diameter) and architecture of the extracellular matrix (ECM) are suggested.[8]

Among ICPs, PANI has gained increasing popularity because of its ease of synthesis,[13] simple doping/dedoping process,[14] high conductivity,[15] and environmental stability. PANI nanofibers were successfully electrospun for the first time by MacDiarmid et al. at the beginning of the millennium. However, because of the poor solubility and low viscosity of the ICP solutions, rarely pure PANI fibers can be electrospun.[16] Usually, PANI-based materials are electrospun in blend with a second polymer (e.g., polystyrene,[17] poly(ethylene oxide) (PEO),[7,18] polymethyl methacrylate (PMMA),[19] nylon-6,[20] poly(vinylidene difluoride),[21] poly(lactic acid),[22] and polyacrylonitrile[23]), with the unique role to assist the fiber formation. Besides poor processing, PANI lacks flexibility and is nonbiodegradable; furthermore, the traditional chemical synthesis based on aniline polymerization produces a carcinogenic pollutant (i.e., benzidine) and it has been reported to induce chronic inflammation in vivo.[24–26] Therefore, concerns still exist regarding its biological applications.

In the last years, efforts have been focused on enhancing PANI biocompatibility by purification after synthesis, presoaking in medium before cell culturing or grafting adhesive peptides.[27] Another approach consists in the development of innovative protocols to produce ICPs by environmentally friendly green approaches.[28] Inspired by the pioneering studies of Genie`s and Kitani,[29,30] we have recently investigated the possibility to produce PANI by oxidative polymerization of N-(4-aminophenyl)aniline (i.e., aniline dimer, AD) using hydrogen peroxide or molecular oxygen as the oxidizing agents, which leads to H_2O as the unique coproduct, and employing inorganic salts or nanoparticles as the catalysts.[31] This approach avoids the use and production of toxic/mutagen substances, such as aniline, metals in high oxidation state as the reagents and benzidine as the coproduct, and simplifies the post-treatment of the polymeric materials, which does not involve a post-production surface polymerization onto the fiber mat.

Recently, a new procedure to produce highly homogeneous PANI nanofibers has been proposed. It exploits a solvent-induced segregation of aniline dimer on a nylon-6 fiber surface during the electrospinning process, followed by an oxidative surface polymerization onto the wire-shaped template.[32] Issues related to the poor processing of PANI are avoided and a remarkable control over the fiber morphology is obtained.

In this work, we present our recent achievements on the optimization of AD oxidative polymerization by H_2O_2/Fe^{+3} system. Taking advantage of the enhanced solubility of the resulting polymer, we have obtained ultrathin and defect-free fibers from the direct electrospinning of a PANI/polymethyl methacrylate (PMMA) solution. The resulting PANI emeraldine shows a relatively good solubility in the organic solvents used for electrospinning. This allowed us to increase the content of the conducting polymer in the feed solution.

Previous investigations using PEO as supporting polymer were not successful in producing uniform PANI fibers. Indeed, optical microscope images of the electrospun fibers show clearly the presence of small dark spots along the fiber, which can be attributed to PANI not uniformly distributed along the fiber (see Supporting Information, Figure 1). Moreover, after rinsing the mat with acetonitrile, the fiber morphology is disrupted and onto the substrate only the dark spots remain. For this reason we did not further proceed with this polymer and we chose PMMA as supporting polymer, which is a valid alternative for its high molecular weight and the possibility to have a segregation between PANI/PMMA along all the fiber axis without using a coaxial electrospinning. The good morphology and uniformity of PANI/PMMA electrospun fibers were maintained even after the removal of the supporting polymer, while in vitro biocompatibility of the resulting mats was assessed with SH-SY5Y neuronal-like cells (without pre-soaking in medium before cell exposure). The results indicated that the tested PANI-based nanofibers do not release any toxic leachable and support cell adhesion and proliferation. In particular, one of the proposed mats does not lower the cell proliferation rate when cells are cultured directly on its surface.

EXPERIMENTAL

Materials

Polymethyl methacrylate (PMMA; M_W = 996,000) dodecylbenzenesulfonic acid (DBSA), N-(4-aminophenyl)aniline (AD), $FeCl_3 \cdot 6H_2O$, hydrogen peroxide (30% w/w), NH_4OH solution 28% w/w, 0.1 M HCl solution, organic solvents, KBr and resazurin sodium salt were purchased from Sigma-Aldrich and used as received. Reagents for cell culture were obtained from Invitrogen™ Corp., while tissue culture plasticware was from Corning and CellTiter 96® AQueous One Solution Cell Proliferation assay (MTS) was purchased from Promega Corp.

N-(4-aminophenyl)aniline (AD) Oxidative Polymerization

400 mg of AD (2.2 mmol) were dissolved in 80 mL of deionized water containing different amounts of 0.1 M HCl. After complete AD dissolution, suitable volumes of H_2O_2 and the appropriate amount of catalyst (aqueous solution of $FeCl_3 \cdot 6H_2O$, $[Fe] = 2.2 \times 10^{-2}$ M) were added very quickly. The resulting mixture was stirred at room temperature for 24 h. Thereafter, a dark green precipitate, characterized as emeraldine salt (ES), was recovered by filtration, thoroughly washed with deionized water and acetone until the washings were nearly colorless and dried in oven at 65 °C for 6 h.

The resulting optimized reaction conditions are: T =23 °C, $[HCl] = 1.36 \times 10^{-1}$ M, $[AD] = 2.72 \times 10^{-2}$ M, $[Fe^{+3}] = 1.67 \times 10^{-5}$ M, $[H_2O_2] = 2.72 \times 10^{-2}$ M, reaction time = 24 h.

Soluble PANI/DBSA Samples Preparation

PANI (700 mg) was dedoped in 10 mL of 0.5 M NH_4OH at room temperature. After 24 h stirring, a dark blue product was filtered, washed several times with water until the mother

Table I. Feed Solutions, Experimental Electrospinning Conditions, and Mean Fiber Diameter

Sample	CHCl/DMF (v/v)	Voltage (kV)	Rate (mL h_{-1})	Diameter (nm)	Morphology
$F_{1:0}$	3:1	25	0.5	—	Beads
$F_{4:1}$	3:1	25	0.5	—	Beads
$F_{3:1}$	3:1	22	0.5	147 ± 40	Fibers with defects
$F_{2:1}$	3:1	20	0.3	65 ± 14	Fibers
$F_{1:1}$	3:1	20	0.3	194 ± 57	Fibers
$F_{0.5:1}$	3:1	15	0.1	550 ± 170	Fibers

$F_{PANI:PMMA}$ represents the weight ratio (w/w) between the two components in the feed solution.

liquors became neutral and dried under air. The resulting emeraldine base (500 mg) was suspended in 20 mL of chloroform ($CHCl_3$) and 890 mg of dodecylbenzenesulfonic acid (AD/DBSA = 1) molar ratio were added. The mixture was stirred for 24 h and then filtered. The green filtered solution containing soluble materials was evaporated under vacuum. Finally, soluble PANI/DBSA was obtained as a dried green powder.

Polymer Fibers by Electrospinning

Feed solutions were loaded in a 2.5 mL syringe with a 22-gauge needle (Hamilton, Gastight model 1002 TLL). The syringe was mounted onto an infusion pump (KDS Scientific, model series 200) which provided a constant flow rate of feed solution to the capillary nozzle. All the experimental runs were performed at room temperature using a bottom-up vertical configuration, with a distance syringe tip-collector of 20 cm. A high voltage was applied between the syringe needle and a grounded collector by a High Voltage Power Supply (Spellman, model SL30P300). Fiber samples were spun randomly onto glass and silicon substrates for further characterization. Electrospun mats for cell growth experiments were produced electrospinning the fibers directly onto thin glass slides. A long collection time was set to have a dense and compact layer.

Different polymer ratios between PANI and PMMA ($F_{PANI:PMMA}$) were prepared and dissolved in a mixture of chloroform and dimethylformamide (DMF) in a ratio 3:1 v/v, in a concentration of 45 mg mL^{-1} considering both PANI and PMMA. Electrospinning voltage and flow rate are reported in Table I.

Analysis of the mean diameter distribution from scanning electron microscopy images was performed on a minimum of 70 measurements with ImageJ software (Rasband, W.S., ImageJ, U. S. National Institutes of Health, Bethesda, MA, http://rsb.info.nih.gov/ij/, 1997–2014).

The supporting polymer could be removed by rinsing with a selective solvent. Two different solvents were used, namely isopropanol and acetone, to test their effectiveness as well as the effect on the mat morphology. Accordingly, the samples were analyzed as spun and after dipping into isopropanol or acetone bath for 30 min.

Characterization

All the polymeric materials were obtained in the form of ES, as it resulted from Fourier transform infrared spectroscopy (FTIR) and UV–vis analyses, in accordance with those reported in the literature.[33,34] FTIR was performed in transmission mode using a Nicolet NEXUS FTIR interferometer (DTGS detector) on fiber membranes deposited onto ZnSe substrate. The Omnic 7.1 software (Thermo Nicolet Instrumentation) was used to analyze the spectra.

The molecular weight distribution of soluble PANI samples was determined by size exclusion chromatography (SEC) using a Shimadzu LC10ADVP HPLC equipped with a refractive index (RI) as the detector. The SEC column was a Phenomenex Phe-nogel 5u 55 A (300 × 4.6 mm^2). All the measurements were carried out at room temperature using ultra-pure DMF as the eluent. The flow rate was set at 0.3 mL min^{-1} and the injection volume was 20 µL. Polystyrene standards were used for calibration.

Micrographs of the electrospun fiber mats were acquired using a high resolution scanning electron microscope (SEM, model LEO 1525). No conductive coating was deposited onto the samples.

Electrical properties were assessed using a standard two-point setup at room temperature with a Keithley 2635A multimeter (dc) and an Agilent E4980A precision LCR meter (from 20 Hz up to 2 MHz), using gold micro-needles placed in direct contact with metal contacts where the self-standing bundle of electrospun fibers were glued. Cycles were collected in the range [0, +10] V.

X-ray diffraction (XRD) analyses were performed using a Rigaku D IIIMAX horizontal-scan diffractometer with Cu Kα radiation.

In Vitro Biological Studies

Cell Culture. SH-SY5Y human neuroblastoma cells (ATCC® code: CRL-2266™) were selected as cell model and $F_{2:1}$ nanofibers (as spun, dipped into isopropanol or acetone) were used as experimental groups. Cells were cultured at 37 °C in a humidified atmosphere with 95% air and 5% CO_2 in high-glucose Dulbecco's modified Eagle's medium supplemented with 10% (v/v) fetal bovine serum, 2 mM L-glutamine, 100 U mL^{-1} penicillin, and 100 µg mL^{-1} streptomycin. They were passaged twice a week, after reaching 70% confluence.

Sample Preparation. $F_{2:1}$ nanofibers were electrospun on standard glass coverslips (13 mm diameter). The substrates were disinfected by dipping into 70% v/v ethanol, placed into 24-well cell culture plates and sterilized by UV irradiation (254 nm, 5 min) or autoclave (Golmar, model NT 80. Temperature > 121 °C, pressure > 1.1 bar, 20 min). To analyze whether the sterilization method affects the fibrous morphology, nanofibers were observed by SEM, as reported.

Elution Assay. The effect of potentially toxic leachable released from the different $F_{2:1}$ fibers on cell survival was evaluated by the elution assay. Cells were seeded in a 96-well cell culture plate at a density of 93,750 cells cm^{22}. After 24 h, culture medium was replaced with 100 mL supernatants, obtained by incubating the nanofibers (sterilized by UV irradiation) with 1 mL culture medium for 1, 3, 7, 10, and 14 days at 37 °C in 5% CO_2. At each time point the supernatants were collected and stored at 4 8C in the dark. As a control group (CTRL), standard culture medium was sampled at the same time points and then added to the cells. After 24 h incubation, the survival rate was assessed by MTS assay. Briefly, 10% v/v MTS was added to culture medium and after 3 h incubation at 37 °C in 5% CO_2, the optical density (OD) was measured at 490 nm (reference wavelength = 630 nm) by a spectrophotometric plate reader (Tecan, model Infinite® 200 PRO).
The OD values measured for the blank group (culture medium only), CTRL group and experimental groups were coded as OD_{blank}, $OD_{control}$ and OD_{sample}, respectively. Cell survival rate (%) in the supernatants sampled at time t was calculated by eq. (1):

$$\frac{ODsample(t) - ODblank}{ODcontrol(t) - ODblank} \cdot 100 = \text{Survival rate (\%)} \quad (1)$$

Cell proliferation on the Nanofibers. The effect of the different $F_{2:1}$ fibers on cell proliferation was investigated by resazurin colorimetric assay. Cells were seeded on the nanofibers (sterilized by UV irradiation) at a density of 37,500 cells cm^{-2} in 1 mL culture medium. As a CTRL group, cells were seeded on standard tissue culture plates. On days 1, 3, 7, 10, and 14 cell proliferation was evaluated by resazurin assay. Briefly, 10% v/v 0.2 mg mL^{-1} resazurin sodium salt in phosphate buffered saline was added to culture medium and after 3 h incubation at 37 °C in 5% CO_2, the fluorescence was measured (excitation wavelength = 560 nm, emission wavelength = 590 nm) by a spectrophotometric plate reader.
The fluorescence values measured for the blank group (culture medium only), CTRL group and experimental groups were coded as F_{blank}, $F_{control}$, and F_{sample}, respectively. Cell proliferation with time (%) was calculated by eq. (2):

$$\frac{Fsample(t) - Fblank(t)}{Fcontrol(t) - Fblank(t)} \cdot 100 = \text{Proliferation rate (t, \%)} \quad (2)$$

Statistics. Experiments were performed on samples from four different sets of electrospun fibers; in particular for *in vitro* biological studies $F_{2:1}$ samples from two different sets were used. Data are reported as mean 6standard deviation (SD). Statistical analysis was performed using GraphPad Prism software, release 6.05. Two-way ANOVA for repeated measurements followed by Dunnett's multiple comparisons test was used for comparisons among the groups and time frames. The significance level was set at p-value < 0.05.

RESULTS AND DISCUSSION

Many different methods have been developed to produce PANI, including chemical, electrochemical, enzymatic ways and numerous other unusual approaches. Although aniline polymerization by stoichiometric oxidants is the most used method, the resulting polymer material appears hard to be processed. As reported by Wei et al., the necessity to employ strong oxidizing agents in large amount is related to thermodynamic limitations,[35,36] since the most energy-demanding step of polymerization is the oxidation of aniline monomer to form dimeric species.

To overcome this issue, recently we have proposed an alternative approach consisting in the oxidative polymerization of AD, a commercially available material. The use of AD allows to replace hard oxidants with greener chemicals (molecular oxygen or hydrogen peroxide) in the presence of proper catalysts.[21,37] Herein, we report the optimization of the reaction conditions for the oxidative polymerization of AD using H_2O_2 and Fe^{+3} as the oxidant and catalyst respectively, to achieve PANI in its conducting form (ES) with high yields. Specifically, a series of reactions were carried out varying catalyst (Fe^{3+}) amount, oxidant (H_2O_2) and acid (HCl) molar concentrations, while maintaining AD molar concentration constant (2.72×10^{-2} M). The results are reported in Table II.

It is worth noting that while increasing the catalyst amount from 6.25×10^{-6} M to 1.25×10^{-5} M the polymerization yield is low and quite constant. At a catalyst concentration of 1.67×10^{-5} M polymerization yield raises up to 55.7%, but it decreases for further increases. Even though the influence of catalyst amount on the polymerization reaction is still not clear, it could be reasonably related to the oxidizing agent decomposition, according to the Fe^{+3}-mediated H_2O_2 decomposition mechanism proposed by De Laat and Gallard.[38]

It was spectroscopically demonstrated that the first step of the reaction between H_2O_2 and Fe^{13} turns into the formation of a Fe-(III)-hydroperoxy complex [$FeIII(HO_2)^{+2}$] or to diperoxo complexes when very high H_2O_2 concentrations are used. The H_2O_2 decomposition reaction seems to be initiated by the unimolecular decomposition of Fe(III)-hydroperoxy complexes.

The authors also observed that H_2O_2/Fe^{+3} molar ratio impacts on the H_2O_2 decomposition kinetic constant. In particular, this latter increases with H_2O_2/Fe^{13} molar ratio up to reach a plateau and, thereafter, decreases. This decrease was attributed to a drop of the molar fraction of uncomplexed Fe(III), responsible for the further decomposition reaction with increasing H_2O_2 concentration.

Although the real mechanism involved in the PANI synthesis by Fe^{13} and H_2O_2 is not completely clear, the mechanism of H_2O_2 decomposition in the presence of Fe^{13} ions to produce radical species could have a key role. According to the literature, some mechanisms have been proposed for aniline monomer polymerization. When AD is used as the reagent, both H_2O_2 and Fe^{3+}

Table II. Dependence of Polymerization Yield on Fe^{31} Catalyst, Acid, and Oxidant Amounts

	$[H_2O_2]/[AD]$	[HCl]/[AD]	$[Fe^{3+}]$ (mol L^{-1})	Yield (%)
Catalyst conc. variation	5	1	6.25×10^{-6}	6.9
	"	"	1.25×10^{-5}	6.9
	"	"	1.67×10^{-5}	55.7
	"	"	2.50×10^{-5}	14.2
	"	"	5.00×10^{-5}	16.1
Acid conc. variation	"	0.5	1.67×10^{-5}	0.5
	"	2	"	66.8
	"	5	"	78.3
Oxidant conc. variation	"	"	"	78.3
	2.5	"	"	88.5
	1	"	"	90.8

Reaction conditions: [AD] = 2.72×10^{-2} M; temperature = 23 °C, reaction time = 24 h. The resulting best conditions are set in bold.

can act as the oxidants from a thermodynamic point of view and also the HO• radical species can contribute to PANI production. This means that all these mechanisms can be involved in the AD oxidative polymerization, as evidenced in Scheme 1, and H_2O_2/ Fe^{+3} molar ratio can play an important role.

A great improvement in the reaction yield was gained by raising the acid amount from the bare minimum needed to obtain PANI in its conducting form (ES) to a five-fold excess (Table II), reaching the best value of 78.3%. In the reaction mixture the acid performs multiple roles. On the one hand the presence of acid is fundamental to increase H_2O_2 oxidizing power, on the other hand it could have a positive effect in the catalyst re-oxidation, neutralizing the HO^2 ions deriving as coproducts from H_2O_2 decomposition (see Scheme 1). Finally, raising the acid amount in the reaction mixture leads to a growth in the Fe(III) complexes, responsible for further H_2O_2 decomposition.

Once fixed the acid concentration (1.36×10^{-1} M) and the catalyst amount (1.67×10^{-5} M), H_2O_2 molar concentration was optimized and the results are reported in Table II.

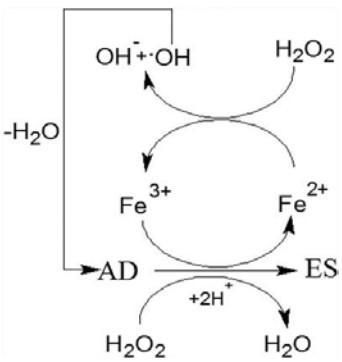

Scheme 1. Scheme proposed for N-(4-aminophenyl)aniline oxidative polymerization to emeraldine salt (ES) with H_2O_2/Fe^{13} system.

A slight polymerization yield improvement was obtained by decreasing H_2O_2 molar concentration from 1.36×10^{-1} M to 2.72×10^{-2} M.

All these materials were characterized by FTIR and UV–vis spectroscopies and the results were in line with those reported in the literature for ES. PANI synthesized under optimized reaction conditions (T = 23 °C, [HCl] = 1.36×10^{-1} M, [AD] = 2.72×10^{-2} M, $[Fe^{+3}] = 1.67 \times 10^{-5}$ M, $[H_2O_2] = 2.72 \times 10^{-2}$ M, reaction time524 h) was treated as reported in Soluble PANI/DBSA Samples Preparation section, thus obtaining a PANI/DBSA soluble fraction which was then processed by electrospinning.

The molecular weight of soluble PANI/DBSA fraction was estimated by SEC using polystyrene standards, obtaining M_w = 38,000 (polydispersity = 1.0). As polystyrene and PANI have different hydrodynamic volumes,[39] these data must be considered as apparent molecular weights and not absolute ones.

To produce fibers, PANI was dissolved in a mixture of chloroform and DMF (ratio 3:1 w/w) with an increasing content of PMMA as the supporting polymer. Even though PANI's solubility is higher in DMF than in chloroform, the high boiling point of DMF (153 8C) can lead to incomplete evaporation of the solvent during spinning. Therefore, to achieve both a complete PANI dissolution and a control over the spinning process, a mixture of DMF and chloroform was used. The obtained PANI from AD oxidative polymerization shows a good solubility in the feed solvent mixture. It is worth noting that attempts to solubilize PANI obtained from the polymerization of the aniline monomer led to a remarkable residue and filtration was required before electrospinning. However, this last step modifies the nominal concentration of the solution. As we could not have control over the resulting concentration, this procedure was ruled out.

The electrospinning of a pure PANI solution has afforded a spray of micrometric particles rather than fibers, as reported in Figure 1(a). The addition of PMMA is necessary to stabilize the electrospinning process and obtain a stable flow and an entangled jet. Solutions with increasing PMMA content were

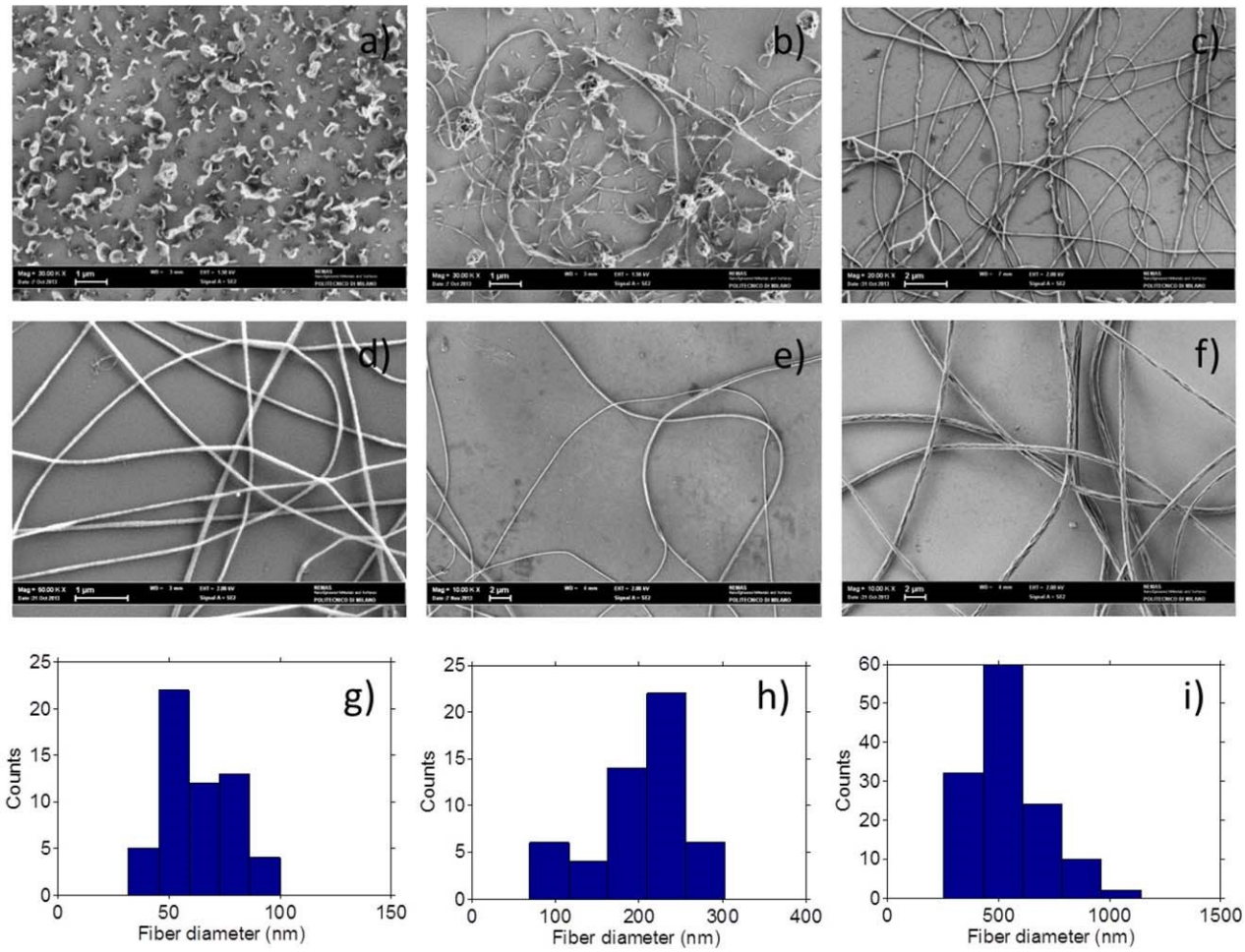

Figure 1. SEM images of electrospun fibers from different feed solutions with an increasing content of PMMA ($F_{PANI:PMMA}$ w/w). (a) $F_{1:0}$, (b) $F_{4:1}$, (c) $F_{3:1}$, (d) $F_{2:1}$, (e) $F_{1:1}$, (f) $F_{0.5:1}$. Frequency distribution of fiber diameter for different defect-free fiber samples. (g) $F_{2:1}$, (h) $F_{1:1}$, (i) $F_{0.5:1}$.

prepared and the results of the electrospinning process are reported in Figure 1. For low PMMA amounts (sample $F_{4:1}$) sprayed particles with incipient fibers were formed, and an esti-mation of the mean diameter was not possible due to the extreme irregularity of the mat. An increasing in PMMA content (sample $F_{3:1}$) led to a less defective situation with no par-ticles spray but beaded fibers with poor homogeneity of the mat [Figure 1(c)]. All the other solutions have afforded defect-free and homogeneous fibers. Solution $F_{2:1}$ has given rise to exceptionally thin fibers (65614 nm, mean diameter) with a remarkable surface and dimensional uniformity. Electrospinning has provided defect-free fibers at reduced voltage and flow rate for a further increase of PMMA in the feed solution ($F_{1:1}$ and $F_{0.5:1}$); under these conditions, the resultant fibers were charac-terized by a higher diameter, up to ten times bigger, as well as by a reduced content of PANI in the final mat.

With respect to previous works, fibers electrospun from a weight ratio of 2:1 between PANI and PMMA ($F_{2:1}$) contained a greater amount of PANI, namely a smaller quantity of support-ing polymer was required to ensure fiber formation. Moreover, $F_{2:1}$ fibers displayed tiny diameters, smaller than most of the examples reported in the literature,[7,17,20,22,23] Only Li et al. have previously presented PANI-gelatin fibers with a comparable section (61 ± 13 nm) for a blend 60:40 v/v.[40]

The XRD pattern of PANI nanofibers ($F_{2:1}$) shows a broad band at 2θ = 20° which indicates that the polymer has an amorphous structure (see Supporting Information Figure 2). This finding is in accordance with the experimental results reported in literature on similar systems.[19,41]

Electrical conductivity measurements onto PANI/PMMA $F_{2:1}$ nonwoven mats were carried out on a bundle of fibers glued with silver paste onto metal electrodes. In the experiments an increasing DC voltage was applied from 0 to 10 V to the metal contacts and then swept back to 0 for several times. The current flowing through the bundle was measured as a function of the applied voltage. An ohmic behaviour of the coating was shown, and by the linear I–V curve and the geometrical dimension of the bundles, the conductivity value of the bundle was obtained.

Three different samples were prepared, and the dimension of the mat was determined by the analysis of optical images.

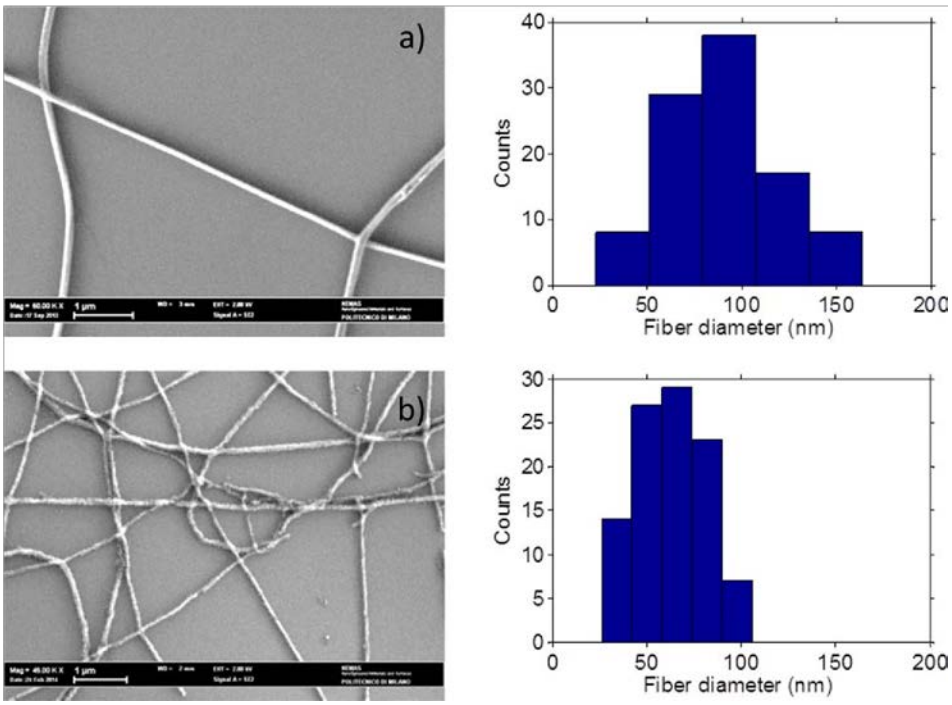

Figure 2. SEM images (left) and frequency diameter distribution (right) for washed electrospun mats $F_{2:1}$. On top: after dipping into isopropanol, mean fiber diameter 86 ± 30 nm. On bottom: after dipping into acetone mean fiber diameter 62 ± 19 nm.

However, this approximation led to an underestimation of the conductivity.

The conductivity of $F_{2:1}$ mats was of $1.8 \pm 0.7 \times 10^{-9}$ S cm^{-1} and this value is in good agreement with analogous PANI mats reported in literature.[42–46]

It is worth noting that the supporting polymer can be removed from these thin fibers by rinsing with a selective solvent while maintaining the fibrous morphology. In this work, isopropanol and acetone were tested.

To monitor the removal of PMMA, $F_{2:1}$ fibers were collected directly onto silicon substrates for SEM measurements and onto ZnSe window for FTIR analysis. Dipping of the spun mat into isopropanol did not affect the morphology of the fibers, which remained homogenous and with a smooth surface [Figure 2(a)]. However, using isopropanol the supporting polymer removal was not complete (as highlighted by FTIR spectra after washing, where the characteristic features of carboxylic acid stretching at 1720 cm^{-1} of PMMA were still present, see Supporting Information Figure 3). Rinsing in acetone, which is a good solvent for PMMA, was effective. The removal of the supporting polymer was almost complete while preserving the fibrous morphology of the spun mat, although the fiber surface appeared more wrinkled. Therefore, after washing in acetone pure conductive PANI nanofibers were obtained.

As a starting point to assess *in vitro* biocompatibility and nerve cell proliferation, as spun–random mats of fibers have been used. Studies focusing on cell differentiation and behavior based on electrical stimulation need to take into account that oriented scaffolds can play a pivotal role.[47,48] For such investigations, undifferentiated SH-SY5Y cells are not the best model. Differentiated SH-SY5Y cells (e.g., via treatment with 10 μM retinoic acid and 1% v/v fetal bovine serum) are a better choice, since they are more likely to neurons and may better respond to electric current.

After preparation, $F_{2:1}$ fibers were sterilized by autoclave (temperature > 121 °C, pressure > 1.1 bar, 20 min) or UV irradiation (254 nm, 5 min), then their morphology was observed by SEM.

Autoclave sterilization is the easiest sterilization method approved by the Food and Drug Administration, but it affects the scaffold geometry and features in the case of easily degradable and noncrosslinked polymers.[49] In contrast, UV irradiation has been reported to sterilize electrospun scaffolds without affecting their chemical and morphological properties. For such structures, hydrogen peroxide gas plasma may also be effective.[50] In the present study, the fibrous morphology was still present after autoclaving, but the nanofibers appeared looser and tighter. On the contrary, following UV exposure fiber morphology resembled the starting one (Figure 3). For this reason, this sterilization technique was selected for the following experiments.

A few studies related to the biocompatibility of pure PANI are available and the results are conflicting and dependent on cell type. For example, H9c2 cardiac myoblasts proliferate on both conductive and non-conductive pure PANI films, but up to 100 h after seeding their doubling time is longer on conductive films than non-conductive films or tissue culture plates. In contrast, the adhesion of PC12 cells is reduced on conductive PANI

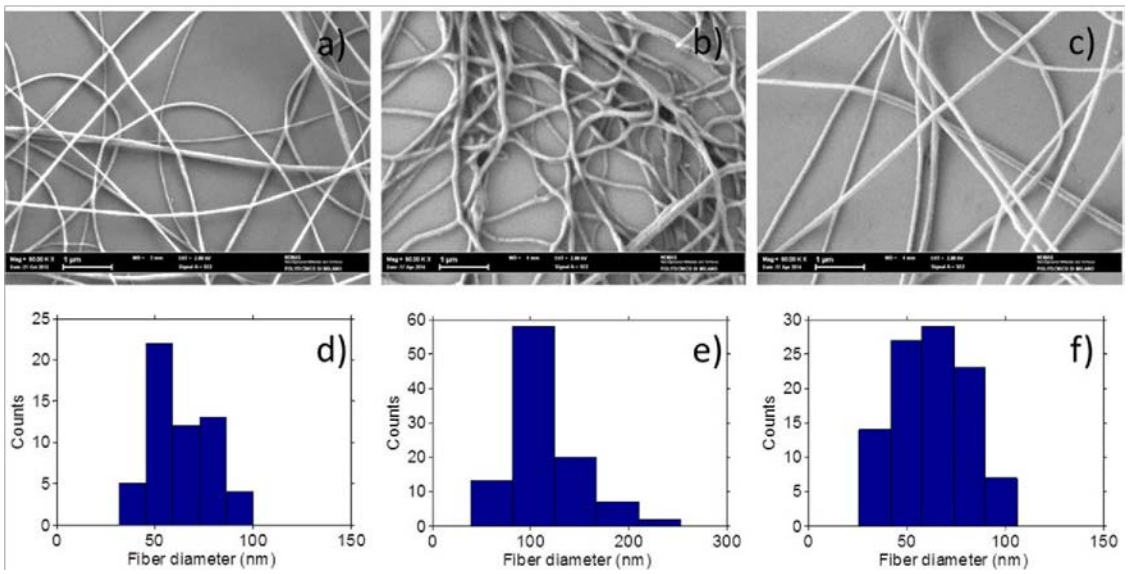

Figure 3. SEM images (top) and frequency diameter distribution (bottom) of $F_{2:1}$ electrospun mats (a–d) as spun, mean fiber diameter 65 ± 14 nm, (b–e) after autoclave sterilization (temperature >121 °C, pressure >1.1 bar, 20 min), mean fiber diameter 113 ± 36 nm and (c–f) after UV sterilization (254 nm, 5 min), mean diameter 76 ± 29 nm.

films.[51] It may be improved by doping the films with acids, that contributes to create a nanoscale topography.[52]
Also blending PANI with other polymers (i.e., gelatin, poly(L-lactic acid-co-e-caprolactone), poly(lactic-co-glycolic acid), or poly(e-caprolactone)) allows to improve pure PANI *in vitro* biocompatibility.[53–56] Because of its advantages in obtaining uniform fibers in the electrospinning process, we have blended PANI with PMMA and tested the in vitro biological performance of the selected $F_{2:1}$ fibers without pre-soaking in medium.

The presence of degradation products which are non-cytotoxic and do not inhibit cell proliferation and functions is a fundamental feature for biomaterials. The results (Figure 4) from indirect tests indicated that cell survival rate in conditioned media was comparable to CTRL in standard medium for all *$F_{2:1}$* fibers at all the sampling time points (p-value >0.05), suggesting that the proposed optimization of AD polymerization allows to obtain soluble PANI electrospun mats free of cytotoxic leachable at both short and longer times. Accordingly, bright-field images (see Supporting Information Figure 4) show that at all the conditions SH-SY5Y cells extend long neuritis and their morphology is similar to CTRL.

Furthermore, the results from direct tests indicated (Figure 5) that for *$F_{2:1}$* fibers dipped into isopropanol cell proliferation rate was comparable to CTRL on tissue culture plate at all the time points (p-value >0.05); while it was reduced on the other substrates. Accordingly, bright-field images (see Supporting Information Figure 5) show that controls extend long neuritis, while a greater number of round-shaped cells was found on *$F_{2:1}$* fibers without PMMA.

The results have suggested that the presence and amount of PMMA are both fundamental; in particular, the amount is

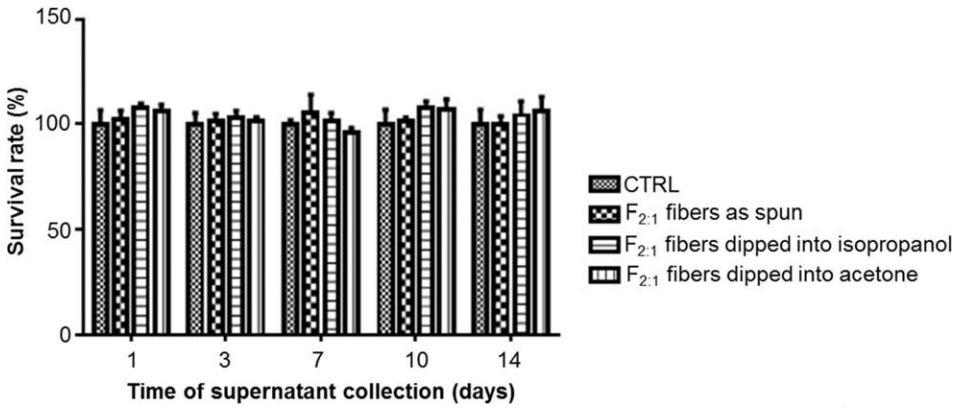

Figure 4. Elution assay. Survival rate of SH-SY5Y neuronal-like cells after incubation with the supernatants collected from *$F_{2:1}$* fibers as spun and dipped into isopropanol or acetone. The results were reported as a percentage with respect to CTRL in standard culture medium sampled as the supernatants (mean ± SD). The results were comparable to CTRL (p-value > 0.05) at all the time points and for all the fiber sets. Statistical analysis was performed by two-way ANOVA for repeated measurements followed by Dunnett's multiple comparisons test.

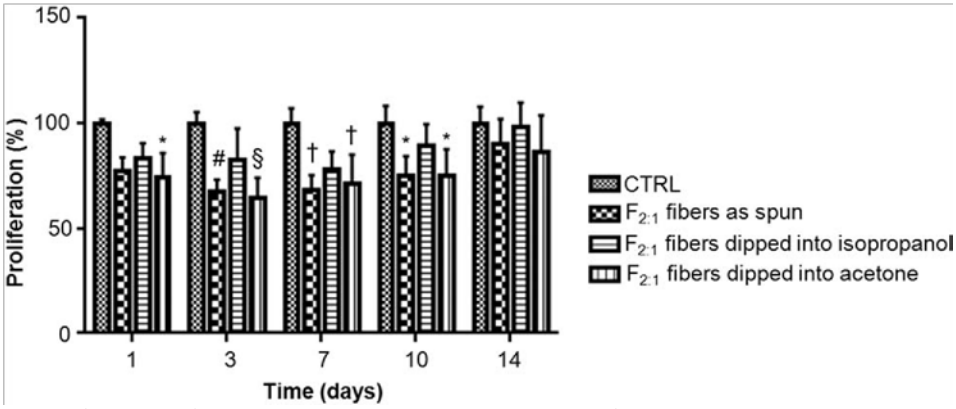

Figure 5. Resazurin assay. Proliferation rate for SH-SY5Y neuronal-like cells cultured on $F_{2:1}$ fibers as spun and dipped into isopropanol or acetone. The results were reported as a percentage with respect to CTRL in standard culture medium (mean6SD). Statistical analysis was performed by two-way ANOVA for repeated measurements followed by Dunnett's multiple comparisons test. * indicates p-value < 0.05; † indicates p-value < 0.01; # indicates p-value < 0.001; while § indicates p-value < 0.0001.

tuneable by selecting a proper solvent for the washing phase. This trend may be explained by considering surface wettability. It is reported that substrates with intermediate wettability (e.g., water contact angles of 40–708) show the best performances. For electrospun mats the ideal range is also influenced by fiber orientation, porosity, diameter and crystallinity. PANI is considered a hydrophobic polymer, but the presence of PMMA increases its wettability by adding polar groups.[55,66] Finally, we may also hypothesize that the results are affected by surface roughness.[57] In fact, SEM images (Figure 2) have suggested that the removal of PMMA leads to more wrinkled fibers, while isopropanol does not change surface topography.

CONCLUSIONS

In the present work we have optimized the N-(4-aminophenyl)aniline oxidative polymerization by H_2O_2/Fe^{+3} system. The relatively high solubility of the resulting PANI has allowed to afford defect-free fibers by electrospinning of a PANI solution containing a relatively low content of supporting polymer (i.e., PMMA). The optimized synthesis procedure affords a PANI polymer with good solubility in the electrospinning solvents. Therefore, we were able to increase the content of PANI in blend with PMMA up to 2:1 w/w, thus obtaining highly uniform and ultrathin electrospun fibers. In the best case, ultrathin and homogeneous electrospun fibers of pure PANI (65 ± 14 nm, mean diameter) have been collected, the thinnest so far reported in literature. It is worth noting that the resulting fiber dimension is in the same range of the native ECM, whose microenvironment is a model for the development of scaffolds with key properties (such as porosity) suitable for cell infiltration and migration. The amount of PANI in the composite fibers was great enough to allow the complete removal of the supporting polymer by washing with acetone, while a partial removal was achieved by isopropanol. Both the solvents have preserved the fibrous morphology. Fibers were also maintained after sterilization, which was effectively carried out with both UV irradiation and autoclaving, with the former method leading to minor effect on morphological features. In vitro biological studies have confirmed that the optimized polymerization conditions lead to non-cytotoxic substrates. In particular, for the optimized nanofibers washed with isopropanol cell proliferation rate was comparable to controls on tissue culture plates at all the time points. Because it is known that they can play a role in regulating differentiation and proliferation of nerve cells, aligned electrospun tissues by PANI/PMMA blend for nerve cell growth will be considered as perspective of the present research.

Such achievements open the way to the use of these fibrous mats as scaffolds for neuronal cells culturing, with the advantage of exploiting direct electrical stimulation to modulate their functions.

ACKNOWLEDGMENTS

The authors gratefully acknowledge financial support by Fondazione Cariplo (Milano, Italy) under grant no. 2012-0872 (Magnetic-nanoparticle-filled conductive polymer composites for EMI reduction).

REFERENCES

1. Wang, W.; Gumfekar, S. P.; Jiao, Q.; Zhao, B. *J. Mater. Chem. C* **2013**, *1*, 2851.
2. Saini, P.; Choudhary, V.; Dhawan, S. K. *Polym. Adv. Technol.* **2012**, *23*, 343.
3. Luo, Y.; Sun, Y.; Lv, J.; Wang, X.; Li, J.; Wang, F. *Appl. Surf. Sci.* **2015**, *328*, 247.
4. Li, J.; Zhao, X.; Zhang, Z.; Lai, Y. *J. Alloys Compd.* **2015**, *619*, 794.
5. Mahmoud, W. E.; Chang, Y. C.; Al-Ghamdi, A.; Al Marzouki, F.; Bronstein, L. M. *Org. Electron. Phys. Mater. Appl.* **2013**, *14*, 2762.
6. Promphet, N.; Rattanarat, P.; Rangkupan, R.; Chailapakul, O.; Rodthongkum, N. *Sens. Actuat. B Chem.* **2015**, *207*, 526.
7. Li, C.; Chartuprayoon, N.; Bosze, W.; Low, K.; Lee, K. H.; Nam, J.; Myung, N.V. *Electroanalysis* **2014**, *26*, 711.
8. Wang, X.; Ding, B.; Li, B. *Mater. Today* **2013**, *16*, 229.

9. Holzwarth, J. M.; Ma, P. X. *J. Mater. Chem*. **2011**, *21*, 10243.
10. Lee, K. W.; Wang, S.; Dadsetan, M.; Yaszemski, M. J.; Lu, L. *Biomacromolecules* **2010**, *11*, 682.
11. Bagherzadeh, R.; Najar, S. S.; Latifi, M.; Tehran, M. A.;Kong, L. J. Biomed. Mater. Res. A 2013, 101 A, 2107.
12. Bagherzadeh, R.; Latifi, M.; Kong, L. *J. Biomed. Mater. Res. A* **2014**, *102*, 903.
13. Syed, A. A.; Dinesan, M. K. *Synth. Met*. **1990**, *36*, 209.
14. Xia, Y.; Wiesinger, J. M.; Macdiarmid, A. G.; Epstein, A. *J. Chem. Mater*. **1995**, *7*, 443.
15. Nalwa, HS. Handbook of Organic Conductive Molecules and Polymers; U.S.A Wiley: **1997**; Vol. 2.
16. Yeh, L.-C.; Dai, C.-F.; Yeh, J.-M.; Hsieh, P.-Y.; Wei, Y.; Chin, T.-Y.; Hsu, M.-Y.; Chen-Yang, Y. W. *J. Mater. Chem. B* **2013**, *1*, 5469.
17. Shin, Y. J.; Kameoka, J. *J. Ind. Eng. Chem*. **2012**, *18*, 193.
18. Frontera, P.; Busacca, C.; Trocino, S.; Antonucci, P.; Faro, M. L.; Falletta, E.; Della Pina, C.; Rossi, M. *J. Nanosci. Nanotechnol*. **2013**, *13*, 4744.
19. Zhao, Y.; Zhang, Z.; Yu, L.; Tang, *Q. Synth. Met*. **2016**, 212, 84.
20. Bagheri, H.; Aghakhani, A. Anal. Chim. Acta 2012, 713, 63.
21. Rose, A.; Raghavan, N.; Thangavel, S.; Uma Maheswari, B.;Nair, D. P.; Venugopal, G. Mater. Sci. Semicond. Process 2015, 31, 281.
22. Abdul Rahman, N.; Feisst, V.; Dickinson, M. E.; Malmstrom, J.; Dunbar, P. R.; Travas-Sejdic, *J. Mater. Chem. Phys*. **2013**, *138*, 333.
23. Zhang, Z.; Zhang, F.; Jiang, X.; Liu, Y.; Guo, Z.; Leng, J. *Fibers Polym*. **2014**, *15*, 2290.
24. Bhang, S. H.; Jeong, S. I.; Lee, T. J.; Jun, I.; Lee, Y. B.; Kim, B. S.; Shin, H. *Macromol. Biosci*. **2012**, *12*, 402.
25. Ghasemi-Mobarakeh, L.; Prabhakaran,M.P,; Morshed, M.; Nasr-Esfahani, Hossein, M.H.; Baharvand, Kiani, S.; Al Deyab, S.S.S.; Ramakrishna, S. *J. Tissue Eng. Regen. Med*. **2011**, *5*, e17.
26. Guarino, V.; Alvarez-Perez, M. A.; Borriello, A.; Napolitano, T.; Ambrosio, L. *Adv. Healthc. Mater*. **2013**, *2*, 218.
27. Qazi, T. H.; Rai, R.; Boccaccini, A. R. *Biomaterials* **2014**, *35*, 9068.
28. Della Pina, C.; Ferretti, A. M.; Ponti, A.; Falletta, E. C*ompos. Sci. Technol*. **2015**, *110*, 138.
29. Genie`s, E. M.; Penneau, J. F.; Lapkowski, M.; Boyle, A. J. *Electroanal Chem. Interfacial Electrochem*. **1989**, *269*, 63.
30. Kitani, A.; Yano, J.; Kunai, A.; Sasaki, K. *J. Electroanal. Chem. Interfacial Electrochem*. **1987**, *221*, 69.
31. Falletta, E.; Della Pina, C.; Rossi, M. *J. Adv. Catal. Sci. Tech nol*. **2014**, *1*, 6.
32. Castagna, R.; Momente`, R.; Pariani, G.; Zerbi, G.; Bianco, A.; Bertarelli, *C. Polym. Chem*. **2014**, *5*, 6779.
33. Basavaraja, C.; Pierson, R.; Huh, D. S.; Venkataraman, A.; Basavaraja, S. *Macromol. Res*. **2009**, *17*, 609.
34. Pan, W.; Qu, L.; Chen, Y. *Optoelectron. Adv. Mater. Rapid Commun*. **2010**, *4*, 2123.
35. Wei, Y.; Jaag, G.-W.; Chan, C.-C.; Hsueh, K. F.; Hariharan, R.; Patel, S. A.; Whitecar, C.K. *J. Phys. Chem*. **1990**, *94*, 7716.
36. Wei, Y.; Tang, X.; Sun, Y.; Focke, W. W. *J. Polym. Sci. A Polym. Chem*. **1989**, *27*, 2385.
37. Chen, Z.; Della Pina, C.; Falletta, E.; Rossi, M. *J. Catal*. **2009**, *267*, 93.
38. De Laat, J.; Gallard, H. *Environ. Sci. Technol*. **1999**, *33*, 2726.
39. Ramamurthy, P. C.; Mallya, A. N.; Joseph, A.; Harrell, W. R.; Gregory, R. V. *Polym. Eng. Sci*. **2012**, *52*, 1821.
40. Li, D.; Frey, M. W.; Baeumner, A. *J. J. Membr. Sci*. **2006**, *279*, 354.
41. Pouget, J. P.; Jozefowicz, M. E.; Epstein, A. J.; Tang, X.; MacDiarmid, A. G. *Macromolecules* **1991**, *24*, 779.
42. Ucar, N.; Kizildag, N.; Onen, A.; Karacan, I.; Eren, O. *Fibers Polym*. **2015**, *16*, 2223.
43. Merlini, C.; Pegoretti, A.; Araujo, T. M.; Ramoa, S. D. A. S.; Schreiner, W. H.; Barra, G. M. D. O. *Synth. Met*. **2016**, *213*, 34.
44. Kizildag, N.; Ucar, N.; Demirsoy, N.; Sezer, E.; Ustamehmetoglu, B.; Eren, O.; Onen, A.; Karacan, I.; Guner, S. *J. Text. Eng*. **2015**, *22*, 1.
45. Wei, M.; Lee, J.; Kang, B.; Mead, *J. Macromol. Rapid Commun*. **2005**, *26*, 1127.
46. Picciani, P. H. S.; Medeiros, E. S.; Pan, Z.; Wood, D. F.; Orts, W. J.; Mattoso, L. H. C.; Soares, B.G. *Macromol. Mater. Eng*. **2010**, *295*, 618.
47. Jiang, T.; Carbone, E. J.; Lo, K. W. H.; Laurencin, C. T. *Prog. Polym. Sci*. **2014**, *46*, 1.
48. Lim, S. H.; Liu, X. Y.; Song, H.; Yarema, K. J.; Mao, H. Q. *Biomaterials* **2010**, *31*, 9031.
49. Runge, B. M.; Wang, H.; Spinner, R. J.; Windebank, A.; Yaszemski, M. J. *Acta Biomater*. **2012**, *29*, 997.
50. Rainer, A.; Centola, M.; Spadaccio, C.; Gherardi, G.; Genovese, J. A.; Licoccia, S.; Trombetta, M. *Int. J. Artif. Organs* **2010**, *33*, 76.
51. Bidez, P. R.; Li, S.; MacDiarmid, A. G.; Venancio, E. C.; Wei, Y.; Lelkes, P. I. *J. Biomater. Sci. Polym. Ed*. **2006**, *17*, 199.
52. Wang, H.; Ji, L.; Li, D.; Wang, J.-Y. *J. Phys. Chem. B* **2008**, *112*, 2671.
53. Huh, J.; Joo, M.-K.; Jang, D.; Lee, J.-H.; Kim, G. T. *J. Mater. Chem.* **2012**, *22*, 24012.
54. Zhang, J.; Qiu, K.; Sun, B.; Fang, J.; Zhang, K.; El-hamshary, H.; Al-Deyab, S.S.; Mo, X. *J. Mater. Chem. B Mater. Biol. Med*. **2014**, *2*, 7945.
55. Hsiao, C. W.; Bai, M. Y.; Chang, Y.; Chung, M. F.; Lee, T. Y.; Wu, C. T.; Maiti, B.; Liao, Z.-X.; Li, R.-K.; Sung, H.-W. *Biomaterials* **2013**, *34*, 1063.
56. Wu, J. C.; Ray, S.; Gizdavic-Nikolaidis, M.; Uy, B.; Swift, S.; Jin, J.; Cooney, R.P. *Synth. Met*. **2014**, *198*, 41.
57. Ribeiro, C.; Sencadas, V.; Areias, A. C.; Gama, F. M.; Lanceros-Mendez, S. *J. Biomed. Mater. Res. A* **2015**, *103*, 2260.